I&EC research
Industrial & Engineering Chemistry Research
pubs.acs.org/IECR
Article

Pilot-Scale Continuous Plug-Flow Hydrothermal Liquefaction of Food Waste for Biocrude Production

Sabrina Summers, Amanda Valentine, Zixin Wang, and Yuanhui Zhang*

Cite This: *Ind. Eng. Chem. Res.* 2023, 62, 12174−12182
Read Online
ACCESS | Metrics & More | Article Recommendations | Supporting Information

ABSTRACT: Pilot-scale hydrothermal liquefaction (HTL) of biowaste is a critical step toward commercialization of the HTL technology. Despite many HTL studies conducted with wet biomass, including food waste, few were performed with a pilot-scale continuous plug-flow reactor (PFR), with the biocrude yield and quality analysis based on dewatering (ASTM D2892 Annex X1). This paper describes the development and performance evaluation of a mobile pilot-scale HTL continuous PFR, with a processing capacity of 60 L/h of wet feedstock and 6 L/h of biocrude production. The reactor system was designed for reaction conditions of up to 325 °C and 17.25 MPa. The reactor has a volume of 28.88 L with an additional counterflow heat exchanger volume of 18.07 L. Two types of food wastes, from a food processing plant and grocery store, were processed at 280 °C for 30 min, producing biocrude oil yields of 52.19 and 47.06 wt %, energy recoveries of 68.17 and 70.77%, and carbon recoveries of 66.91 and 64.78%, respectively. Due to its high feedstock capacity and reaction volume, large amounts of biocrude oil and post-HTL wastewater (PHW) were obtained from this pilot-scale reactor to allow downstream research on upgrading biocrude oil for transportation fuel as well as PHW treatment and nutrient recovery.

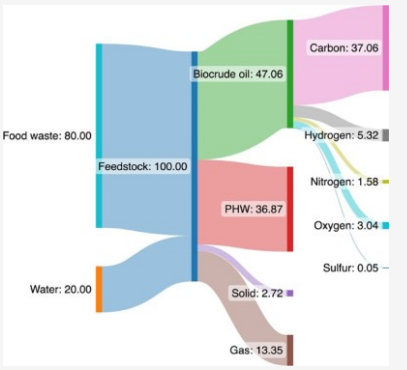

1. INTRODUCTION

Rising human population and technology advancements have presented global challenges, such as increased energy demand and sustainable management of biowaste. The United States produces 77 million dry tons of biowaste annually from the food system alone.[1] This biowaste has been treated as a burden bearing a negative cost. On the other hand, these waste streams have a high content of energy and nutrients that can be recovered and reused. Hydrothermal liquefaction (HTL) is especially suitable for valorization of wet biowaste.[2−4] Without the need for a drying step, HTL is applicable across a wide range of high-moisture content feedstocks including sewage sludge, algae, lignocellulosic material, food waste, and swine manure.[5−7]

HTL is performed at elevated temperatures (250−400 °C) and pressures (4−22 MPa),[8,9] with retention times of 1 to 60 min.[5] Within these ranges, water, a subcritical liquid, acts comparably to polar solvents such as ethanol, methanol, and acetone.[10] Although biocrude is produced with appreciable yields (20−83%) and higher heating values (28−40 MJ/kg), it is of lower fuel quality in comparison to petroleum crude, with high oxygen contents (8−20%).[5,11] Along with biocrude oil, posthydrothermal wastewater (PHW), solid phase, and gaseous phase are also produced during HTL. Composition of these products is dependent on both the compositions of biomass feedstocks (biochemical composition and solid content) and HTL reaction conditions (temperature, pressure, and retention time), making optimization of process parameters a particularly important area of research in the development of this technology.

At the bench scale, both batch and continuous-flow reactors have been used for the HTL process. In the last two decades, most HTL work has been performed in laboratory-scale batch reactors.[12] Using a feedstock of DDGS (dried distiller grain with solubles) at 350 °C, Biller et al. obtained biocrude yields of 34.5 and 44.3 wt % for batch and continuous-flow HTL reactors, respectively.[13] The improved yield from the continuous HTL reactor was attributed to multiple reasons: a higher temperature achieved, improved mixing, and better product recovery. Batch reactor systems for HTL are common for research purposes because it is easier to maintain and control high temperature and pressure process conditions compared to continuous systems. Moreover, batch HTL systems can process feedstocks with higher solid content since pumping and clogging of the reactor are not concerns. However, batch reactors require purging headspace for an inert environment, which would increase operation costs at a full scale. Continuous-flow systems are better suited for pilot- and full-scale HTL processes, with more effective mixing,[13] higher

Received: May 11, 2023
Revised: July 17, 2023
Accepted: July 18, 2023
Published: July 28, 2023

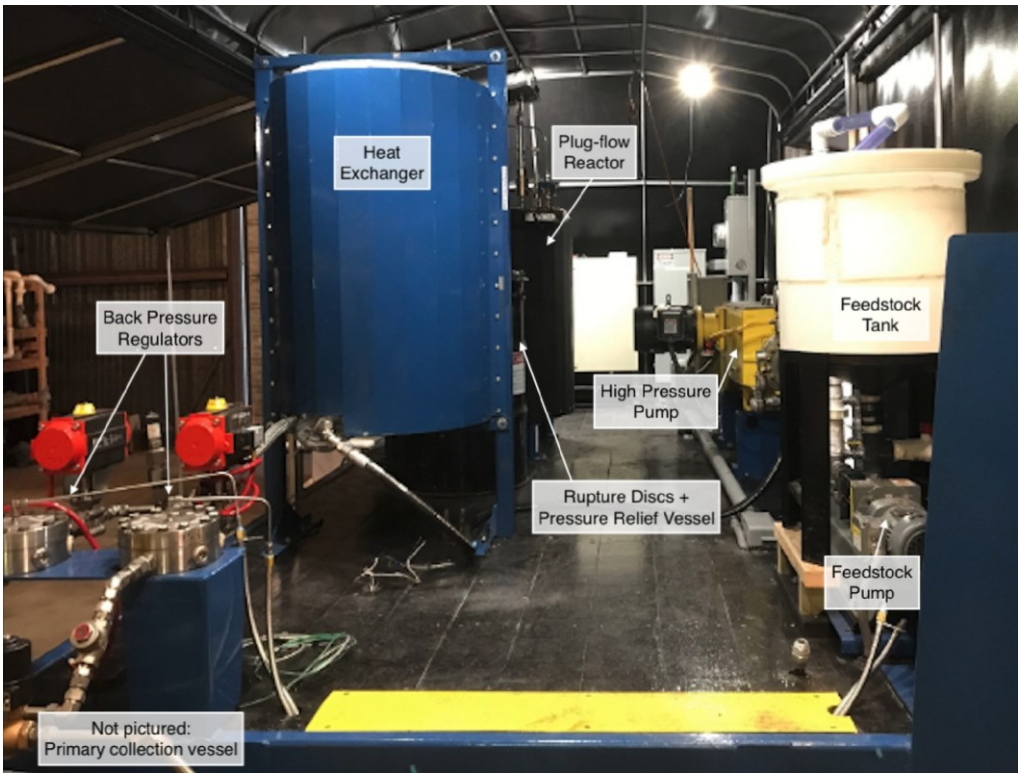

Figure 1. Pilot-scale HTL system on a mobile trailer (inside view).

heating[14] and recovery rates,[13] and increased biocrude yields.[13] However, challenges such as plugging and charring within the system, pressure control and safety, and complex component design have hindered pilot- and full-scale development.[14,15]

Products derived from pilot-scale HTL of wet biomass have numerous potentials, including transportation fuels, biobased chemicals, biogas production, and biobinders for applications such as asphalt.[16,17] For example, polyurethane,[18] resin,[19] and adhesive[20] from HTL biocrude have been formulated. The PHW can be recycled for future liquefaction processes, and nutrients can be recovered for algae and agricultural production, which can generate biogas like hydrogen and methane.[16,21] HTL biochar can also be utilized in soil remediation, carbon sequestration, catalyst supports, and other adsorbent applications.[16]

An extensive review of both historical and recent pilot-scale liquefaction systems in research was completed by Castello et al.[22] The earliest reports of pilot-scale HTL processes were developed at the Albany Biomass Liquefaction Experimental Facility, Lawrence Berkeley National Laboratory, and Hydrothermal Upgrading (HTU) plant in the Netherlands in the 1970s and 1980s.[6] HTL research is continuing to move toward pilot-scale technology, with multiple groups in academia and industry demonstrating significant progress for pilot-scale reactors within the past 10 years, covering biomass feedstocks from lignocellulosic to high-protein-content wet wastes.

The current pilot-scale reactor was developed based on a literature review and the University of Illinois Urbana−Champaign (UIUC) team's own experience on HTL of biomass waste, from batch to continuous and from lab scale to pilot scale. HTL of biowaste aims at not only producing biocrude oil but also mitigating the negative environmental effects of conventional biowaste disposal, such as greenhouse gas emissions and leachate during degradation in landfills.[23] In 2000, He et al.[24−27] reported conversion of swine manure into biocrude oil with a lab-scale batch reactor. Based on the batch test, Ocfemia et al.[28,29] developed and evaluated a continuous stirred tank reactor with a processing capacity of 2 L/h to convert swine manure into biocrude oil. Minarick et al.[30] then developed a plug-flow HTL reactor and analyzed the performance and economic perspective based on the conversion of manure and algal biomass. Aierzhati and the UIUC group then collaborated with an industry partner and developed a plug-flow continuous reactor[31] with a processing capacity of 34 L/h biowaste.

Despite tremendous efforts made in pilot-scale HTL reactor development, there is still a lack of performance data for commercial reactor development. Of all types of HTL reactors investigated, continuous plug-flow has apparent advantages including better mixing, improved heating, and increased biocrude oil yields. However, challenges that arise such as charring and plugging during scale-up restrict pilot-scale development. This paper describes the development and performance of a mobile, pilot-scale continuous plug-flow HTL reactor uniquely operated at a larger reaction volume, higher feedstock solid content, and more moderate temperature. This system is one of the largest existing mobile HTL reactors for published pilot-scale work. Its unique mobility feature allows for a decentralized energy network, along with the cost mitigation of transporting low-energy-density feedstocks.[31] The biocrude oil yield and quality were comparable to those of other pilot-scale HTL work performed in the literature under more severe conditions, proving the feasibility for this operation at commercial applications.

2. MATERIALS AND METHODS

2.1. Pilot-Scale Reactor Development. The current pilot-scale continuous HTL reactor system (Figure 1) is an

https://doi.org/10.1021/acs.iecr.3c01587
Ind. Eng. Chem. Res. 2023, 62, 12174−12182

upgrade of the system described in a previous study.[32] It has the capacity to process 1.5 tons of biowaste and produce 200 L of biocrude oil per day, with potential for further scalability. The process flow diagram for the system (Figure 2) shows its

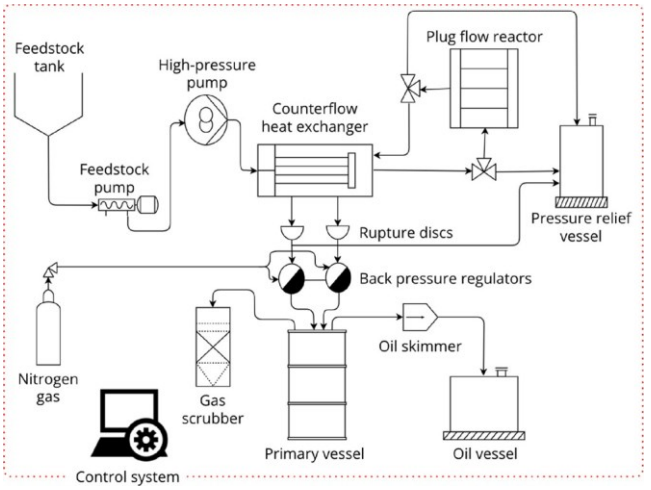

Figure 2. Process flow diagram of the pilot-scale continuous plug-flow HTL reactor system.

process control and monitoring, potable water, feedstock, nitrogen gas, biocrude oil, PHW, and emission routes. Major system upgrades were performed, including replacement of all carbon-steel components with stainless steel, increased reactor volume, increased temperature and pressure ratings, and the addition of a counterflow heat exchanger. It also has an increased biowaste processing capacity of 1.0 L/min. This new pilot-scale HTL system consists of a feedstock tank and pump, high-pressure pump, counterflow heat exchanger, plug-flow reactor (PFR), rupture discs and pressure relief vessel, and back-pressure regulators.

The feedstock tank, feedstock pump, and high-pressure pump store and deliver the feedstock into the reactor system. The feedstock vessel (conical bottom polyethylene holding tank) was relocated from a previously adjacent position to directly above the feedstock pump to allow guaranteed flow of more viscous feedstock into the adjoining feedstock pump. The feedstock pump, a progressive cavity metering pump (Netzsch Nemo Mini BY, Pennsylvania, USA), was controlled by a variable frequency drive (Hitachi model L100). To avoid plugging the high-pressure pump, excess feedstock was continuously recirculated back into the feedstock vessel to prevent accumulated back pressure while being delivered to the high-pressure pump. The high-pressure pump, a positive displacement piston, and a diaphragm pump by Milton Roy (Pennsylvania, USA) delivered feedstock at a high pressure (up to 17.25 MPa) to the counterflow heat exchanger.

The reactor core was composed of a 103.6 m helical coil made of 316L stainless steel (SS), with a reactant volume of 28.88 L. The SS was a Schedule 80 pipe with a 34 in. nominal diameter (1.88 cm inner diameter) and an average flow velocity of 6.00 cm/s. 316L SS was selected because it has lower carbon content than 316 SS and provided improved corrosion resistance. The reactor core was divided into seven heating zones, each wrapped with heat transfer putty (TRACIT-600A, Chemax MFG Corp.) and Mica Band electric heaters (3000 W, 240 V, one-phase), with each heater individually controlled by J-type thermocouples (McMaster-Carr 2860K211). The reactor core was insulated with a ceramic fiber (Unitherm CF8-1-48X25) and a steel jacket. The counterflow heat exchanger was made of the same Schedule 80, 1.88 cm inner diameter 316L stainless steel as the reactor, with a double-screw helical coil 64.9 m in length and 18.07 L volume. The system's temperature control and data logging unit (National Instruments FieldPoint FP-1000 Network Interface) were controlled with LabVIEW.

Pressure within the system was monitored by several devices, including a pulsation dampener, fluid accumulator, rupture discs, pressure relief vessel, exhaust vessel, and back-pressure regulator (BPR). The pulsation dampener (Flow-guard LTD FG54256/02-2) is charged with N_2 gas, and it absorbs the impact of the high-pressure pump stroke and lowers the intensity of pulsations delivered to the reactor. The fluid accumulator (Reasontek RAS-02C3B01NW) is also charged with N_2 gas and was used to maintain system pressure if the high-pressure pump should fail to cycle for a limited duration. A pair of burst rupture discs (Fike 1932613) are housed in an enclosure to relieve pressure from the system automatically in the event of an overpressure scenario. They are connected to the pressure relief vessel and also have a manual pressure relief valve that can be used without breaking the discs. If the system pressure exceeds the disc pressure rating, then the material would be routed to a 55-gallon pressure relief vessel, which collects and retains the solids and then directs gas to a scrubber to catch larger particulate matter and then through activated carbon (Darco 12 × 40) to absorb volatile organic compounds. The set point pressure inside the reactor was regulated by BPRs (Equilibar EQ-4557). A primary vessel collects the HTL products with a belt oil skimmer to separate oil after gravitational settling, and solids in each product stream were filtered out with a bag filter.

2.2. Feedstock Collection and Characterization. Two types of food waste were processed using this pilot-scale HTL reactor: grocery food waste (GFW) from a local grocery store and salad dressing waste (SDW) from a local food processing plant. The GFW was collected at the designated disposal bin, and SDW was collected at a terminal waste tank at the food processing plant. The food processing plant processes up to 1500 tons per day and generates approximately 80 tons of waste per day. A comprehensive characterization of each feedstock was carried out to determine the biochemical composition (Table 1). Proximate analysis and elemental content of the HTL food waste feedstock were done by Midwest Laboratories (Omaha, NE). Methods from the Association of Official Agricultural Chemistry (AOAC) were used to determine protein (AOAC 990.03), lipid (AOAC 945.16), ash (AOAC 942.05) content, and carbohydrate content by difference. The higher heating value (HHV) of the feedstock was calculated from elemental analysis based on eq 1 for Dulong's formula:[14]

$$\mathrm{HHV} = 0.3516 \times \mathrm{C} + 1.16225 \times \mathrm{H} - 0.1109 \times \mathrm{O} + 0.0628 \times \mathrm{N} \quad (1)$$

Physical pretreatment consisted of homogenization with a food processor, grinding through a 16-mesh sieve to obtain a uniform particle size, and dilution with water to reach 20 wt % solid content. The final dilution was completed 1 day before HTL runs, and no separation was observed between the feedstock and water.

https://doi.org/10.1021/acs.iecr.3c01587
Ind. Eng. Chem. Res. 2023, 62, 12174−12182

Table 1. Biochemical Composition of HTL Feedstocks on a Dry Weight Basis for GFW and SDW

characteristic	GFW	SDW
moisture (%)	66.73	75.66
dry matter (%)	33.27	24.34
protein (%)	32.76	2.38
lipid (%)	29.10	62.45
ash (%)	7.15	5.71
carbohydrate [a] (%)	30.99	29.46
carbon (%)	55.38	60.94
hydrogen (%)	7.69	8.27
nitrogen (%)	5.62	0.70
oxygen[a] (%)	27.21	27.45
sulfur (%)	0.33	<0.01
phosphorus (%)	0.60	0.08
potassium (%)	0.87	0.29
magnesium (%)	0.06	<0.01
calcium (%)	0.48	0.08
sodium (%)	1.74	2.16
iron (ppm)	43.90	44.40
manganese (ppm)	7.5	6.2
copper (ppm)	<1.0	<1.0
zinc (ppm)	40.6	5.8
HHV (MJ/kg)[b]	25.74	28.04

[a]Calculated by difference. [b]Calculated by Dulong's formula.

2.3. HTL Reactor Operation. HTL was carried out at a reaction temperature of 280 °C, a pressure of 12.4 MPa, and a retention time of 30 min. Since density was not considered in this study, the residence time distribution (RTD) was simplified to be the RTD of flow in the whole PFR system at the reaction temperature, regardless of any nonuniform temperature profiles. To avoid plugging and charring in the reactor, the capacity and frequency of the high-pressure pump were adjusted to maintain a feedstock flow rate of at least 1 L/min throughout the run. First, the HTL operation was preheated with water; then, once the PFR reached the reaction temperature, the feedstock was introduced. All HTL products were collected in a primary vessel immediately after exiting the BPR. At the end of the feedstock run, water was again flushed through the system to cool down. After products in the primary vessel had gravitationally settled, the biocrude oil was skimmed and then the PHW and biocrude oil were filtered to recover solids.

2.4. Biocrude Oil Dewatering. The HTL biocrude oil was dewatered according to ASTM D2892 Annex X1, "Practice for Dehydration of a Sample of Wet Crude Oil".[33] The biocrude oil was weighed in an SS flask and attached to the distillation column. The biocrude oil was continuously stirred with a stir bar and heated to a vapor temperature of 130 °C, with a reflux ratio = 0. The condenser was vented through two traps maintained at the temperature of dry ice, collecting fractions distilled below 65 °C.

2.5. HTL Conversion Performance and Product Analysis. The HTL performance was evaluated based on mass yield (M_x), energy densification (I_{ed}), energy recovery (E_r), and carbon recovery (C_r):

$$M_x = \frac{m_x}{m_f} \quad (2)$$

$$I_{ed} = \frac{HHV_b}{HHV_f} \quad (3)$$

$$E_r(\%) = I_{ed} \times M_b \quad (4)$$

$$X_r(\%) = \frac{X_b}{X_f} \times M_b \quad (5)$$

where m_x = the dry, ash-free (DAF) mass of the product, where x = b (biocrude), w (PHW), s (solids), or g (gas);
m_f = the DAF mass of feedstock;
HHV_b = the higher heating value of biocrude oil;
HHV_f = the higher heating value of feedstock;
X_r = the DAF basis elemental recovery of biocrude oil, where X = C (carbon), N (nitrogen), or O (oxygen);
X_b = the DAF carbon content of biocrude oil; and
X_f is the DAF carbon content of feedstock.

The product mass balances were conducted as a whole on each batch of oil from the feedstock. The biocrude oil mass was measured after dewatering, and the PHW yield was a combination of the initial water collected from the run and water removed during dewatering. The solid yield was measured by residue filtered out of the biocrude oil and PHW, and the gas yield was obtained by difference.

The elemental composition (carbon, hydrogen, or nitrogen) was measured using an Exeter Analytical Model CE440 CHN analyzer (Coventry, UK), sulfur was measured using a PerkinElmer ICP-MS (Model NexION 350D), and oxygen was calculated by difference. HHV was calculated according to the Dulong formula[14] in eq 1 based on the elemental analysis. The total acid number (TAN) was measured by titration according to ASTM D974[34] using 0.1 M potassium hydroxide and phenolphthalein indicator. Density was determined using a 2 mL glass Gay-Lussac bottle (Core-Palmer, EW-34580-40) at 20 °C. Thermal properties and boiling point distribution[35] were obtained with a TA Instruments Q50 thermogravimetric analyzer (New Castle, DE, USA). During each experiment, the sample (15 mg) was heated from 20 to 700 °C at a rate of 20 °C/min under a N_2 flow rate of 60 mL/min. Chemical characterization of the biocrude oil was conducted with gas chromatography−mass spectrometry (GC−MS) (Agilent Technologies, CA, USA). The sample (2 μL) was injected in split mode to the GC−MS system consisting of an Agilent 6890 chromatograph, an Agilent 5973 mass detector, and an Agilent 7683B autosampler. A 60 m ZB-5MS column of 0.32 mm nominal diameter and 0.25 μm film thickness was used to separate the analyte. The injection temperature was 250 °C, with an initial oven temperature of 70 °C that was increased to 200 °C at a heating rate of 5 °C/min. The source temperature was 230 °C, the electron ionization voltage was 70 eV, and the spectra were scanned from 30 to 800 m/z and evaluated with the AMDIS (NIST, Gaithersburg, MD) program, with all peaks compared to the spectra from the NIST Mass Spectral Database (NIST08).[36] The detailed GC−MS procedure was previously described.[32]

3. RESULTS AND DISCUSSION

3.1. Feedstock Characterization. Although GFW and SDW are both food wastes, they have quite distinct properties. The GFW had a balanced composition of protein (32.76%), lipid (29.1%), and carbohydrate (30.99%), which can be considered as typical restaurant or household food waste.[31,37] On the other hand, the SDW contained little protein (2.38%),

https://doi.org/10.1021/acs.iecr.3c01587
Ind. Eng. Chem. Res. 2023, 62, 12174−12182

high lipid (62.45%), and moderate carbohydrate (29.46%), representing a more particular food waste feedstock. Evidently, food waste biochemical compositions vary largely with their sources.[1] Both feedstocks had low ash contents (5.71−7.15%), which helped to prevent charring upon heating in the reactor.

3.2. Product Collection and Biocrude Oil Dewatering. biocrude oil separated from PHW via gravity and an oil skimmer still contains various amounts of water (Figure 3).

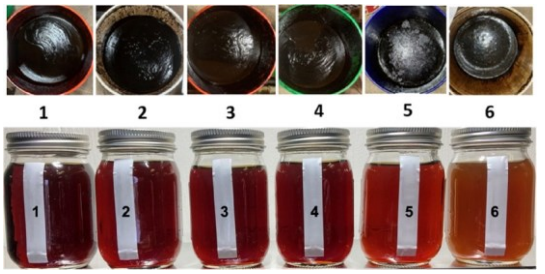

Figure 3. Separated biocrude oil (upper buckets) and PHW (bottom jars). The numbers indicate the sampling pairs and sequence.

Thermogravimetric analysis (TGA) of oil samples shows clear variations among six samples (Figure 4) for each of the GFW and SDW HTL biocrude oils before dewatering pretreatment. These variations demonstrate that separation of biocrude oil and PHW was not consistent along the time of the HTL process. During the HTL run, the output of the HTL reactor was observed to be not homogeneous, with quantity of oil and water in the product composition continuously varying. Therefore, it is critical to dewater the biocrude oil prior to physicochemical characterization.

Water content in the biocrude oil can significantly skew the analysis of the oil property. Figure 5 shows the boiling distribution difference before and after dewatering of the biocrude oil produced from GFW. Prior to dewatering, the light fraction shown as a gasoline category was much higher in the biocrude oil due to the remaining water after the initial separation (Figure 5a). After the dewatering was completed, the light fraction of biocrude oil was much lower, with the water removal resulting in a more uniform boiling point distribution (Figure 5b). Since the dewatering method was conducted up to a vapor temperature of 130 °C, a small quantity of light fraction of biocrude oil was inevitably

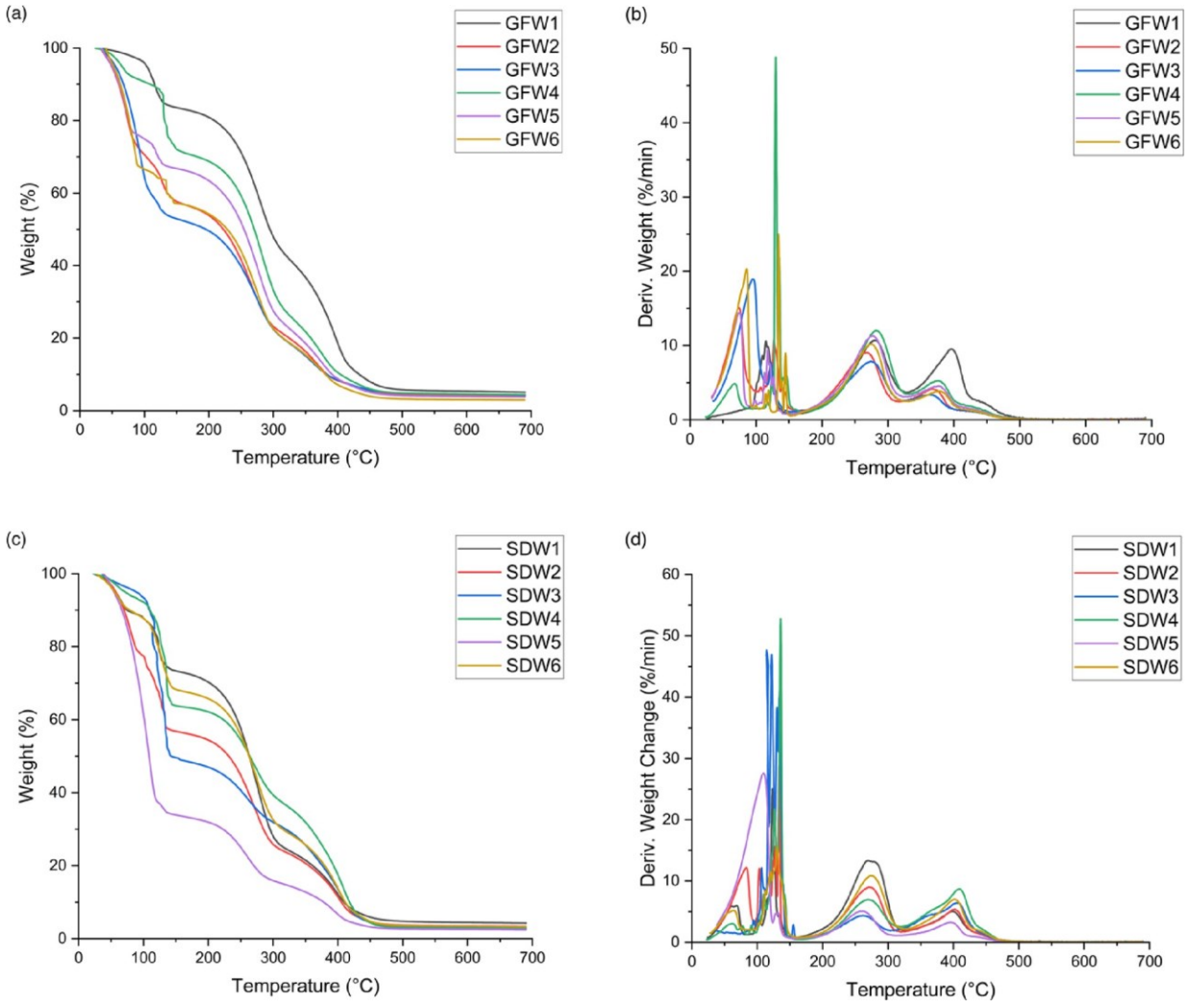

Figure 4. TGA of the raw biocrude oil before dewatering pretreatment: (a) weight change for GFW; (b) derivative weight change for GFW; (c) weight change for SDW; (d) derivative weight change for SDW.

https://doi.org/10.1021/acs.iecr.3c01587
Ind. Eng. Chem. Res. 2023, 62, 12174−12182

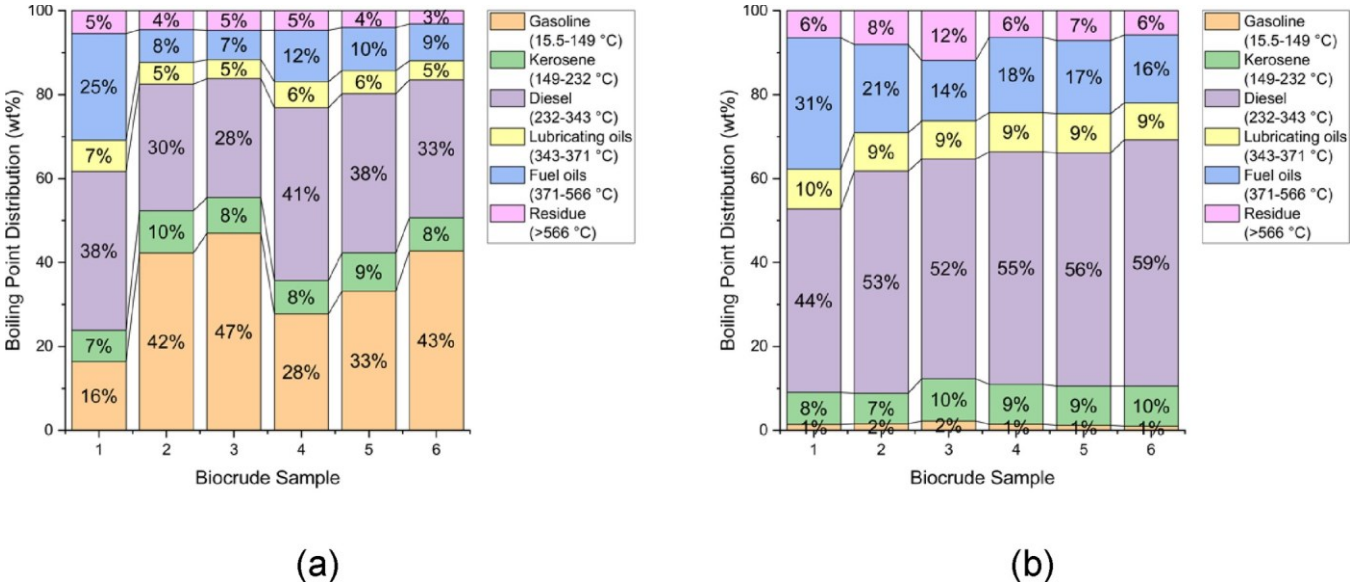

Figure 5. Effect of dewatering on the boiling point distribution property of six GFW biocrude oil samples (a) before dewatering and (b) after dewatering.

evaporated with water; thus, the dewatered biocrude oil yield may be lower than its actual yield.

3.3. HTL Conversion Performance. The performance of the pilot-scale HTL reactor using two types of food waste is summarized in Table 2. The mass yields of HTL products from each feedstock were relatively similar, obtaining biocrude oil yields of 47−52 wt %, PHW yields of 29−37 wt %, solid yields of 1−3 wt %, and gas yields of 13−18 wt %. The higher biocrude oil yield from SDW was a result of the feedstock's higher lipid content (62.45%) compared to GFW (29.10%). Lipid content has been previously shown to have the most impact on HTL conversion efficiency with respect to biochemical composition.[38] The energy densification ratio was 1.45 and 1.36 for GFW and SDW, respectively. Energy densification >1 demonstrated the effectiveness of HTL at these conditions to improve the energy density of each food waste.

Table 2. HTL Conversion Efficiency

	GFW	SDW
M_b (wt %)	47.06	52.19
M_w (wt %)	36.87	29.25
M_s (wt %)	2.72	1.00
M_g (wt %)	13.35	17.56
I_{ed}	1.45	1.36
E_r (%)	68.17	70.77
C_r (wt %)	66.91	64.78
N_r (wt %)	28.14	56.66
O_r (wt %)	11.17	23.12

Both feedstocks produced biocrude oil with similar energy and carbon recovery: 68.17% and 66.91 wt % for GFW and 70.77% and 64.78 wt % for SDW, respectively. However, significant differences were observed in the retention of undesirable heteroatoms, oxygen and nitrogen. While biocrude oil derived from GFW retained just 28.14 and 11.17 wt % of nitrogen and oxygen, the SDW biocrude retained about twice the amount. This may be attributed to the high lipid content in SDW; trends in nitrogen retention and biochemical composition of feedstock have been found with increased biocrude nitrogen recovery with respect to increased lipid content.[4,39] Moreover, some long-chain N-heterocyclic compounds can be produced between lipids and Maillard reaction products.[39] High lipid content in the SDW feedstock may also result in higher oxygen retention in biocrude oil. Subcritical water conditions during HTL lead to the solubility and hydrolysis of lipids, resulting in large amounts of long-chain fatty acid oxygenates.[40]

3.4. HTL Biocrude Oil Properties. The dewatered biocrude oil properties were determined primarily from the point of view of transportation fuels. The biocrude oil quality was determined by physicochemical properties such as the elemental composition, HHV, TAN, and density (Table 3).

Table 3. Physicochemical Characteristics of HTL Biocrude Oil

property	GFW	SDW
carbon (%)	78.74 ± 0.11	75.64 ± 0.02
hydrogen (%)	11.31 ± 0.02	11.42 ± 0.25
nitrogen (%)	3.36 ± 0.01	0.76±0.07
oxygen[a] (%)	6.46 ± 0.14	12.16 ± 0.30
S (%)	0.12	0.01
H/C (mol:mol)	1.72 ± 0.00	1.81 ± 0.04
N/C x10 (mol:mol)	0.36 ± 0.00	0.09 ± 0.01
O/C (mol:mol)	0.06 ± 0.00	0.12 ± 0.00
HHV[b] (MJ/kg)	40.32 ± 0.07	38.57 ± 0.32
TAN (mg KOH/g)	140.66 ± 4.20	132.04 ± 8.54
density (g/mL)	0.95 ± 0.00	0.93 ± 0.00

[a]Calculated by difference. [b]Calculated by Dulong's formula.

The PHW characterization is listed in Table S1. HTL biocrude oil from both feedstocks had similar carbon contents of 78.74 ± 0.11 and 75.64 ± 0.02% for GFW and SDW, respectively, indicating effective carbon recovery efficiency for the pilot-scale HTL process. The biocrude oils also had similar hydrogen contents (11.31 ± 0.02 and 11.42 ± 0.25%, respectively), but there were large differences in the nitrogen

https://doi.org/10.1021/acs.iecr.3c01587
Ind. Eng. Chem. Res. 2023, 62, 12174−12182

and oxygen content. The GFW biocrude oil had a nitrogen content of 3.36 ± 0.01%, while SDW biocrude oil had only 0.76 ± 0.07%. This can be attributed to the original feedstock composition, where GFW had a protein content of 32.76% compared to SDW with 2.38%. The oxygen content of GFW biocrude oil was 6.46 ± 0.14%, while SDW had a higher amount of 12.16 ± 0.30%, attributed to the higher amount of unsaturated fatty acids. To remove undesirable heteroatoms like oxygen, nitrogen, and sulfur, further upgrading of the HTL biocrude oil products, such as hydrotreating, is required to achieve drop-in transportation fuel quality.[32] The HHV of the biocrude oils was 40.32 ± 0.07 MJ/kg for GFW and 38.57 ± 0.32 MJ/kg for SDW. The lower HHV for SDW biocrude oil was due to the increased oxygen content. The TAN of the GFW biocrude oil was 140.66 ± 4.20, while that of SDW biocrude oil was slightly lower at 132.04 ± 8.54, due to the difference in fatty acid contents.

Boiling point distribution is one of the most important indicators for the fuel refining industry. For each of the biocrude oil samples, the boiling point distribution was determined using TGA in a nitrogen atmosphere (Table 4 and Figure 7b).

Table 4. Boiling Point Distribution of the HTL Biocrude Oil

		wt %	
distillate range (°C)	oil type	GFW	SDW
15.5−149	gasoline	1.70	0.91
149−232	kerosene	7.54	6.08
232−343	diesel	52.46	46.17
343−371	lubricating oils	9.14	7.39
371−566	fuel oils	22.69	37.26
>566	residue	6.47	2.19

Six distillate fractions[35] were identified as fuel ranges and are listed in Table 4. It was found that each of the biocrude oil samples had similar boiling point distributions with bimode weight loss peaks. In Figure 6, two major DTG peaks occurred around 300 and 400 °C in both biocrude oils, corresponding to the largest distillate ranges in Figure 7b of diesel (232−343 °C) and fuel oils (371−566 °C). While the DTG peak at 300 °C was largest for GFW biocrude oil, the SDW biocrude oil's larger peak was at 400 °C, indicating a higher amount of heavy fuel oils. Since SDW had a higher amount of lipids in the feedstock compared to GFW (62.45 and 29.10 wt %, respectively), repolymerization reactions may have been favored, leading to production of heavier biocrude oil.[41] Hydrocracking may be a suitable upgrading pathway to convert larger hydrocarbons in the lubricating and fuel oil range into lighter fractions like diesel, kerosene, and gasoline, thereby increasing the amount of lower-molecular-weight compounds.

To elucidate the chemical compositions, Figure 7a,b presents the biocrude oil components as a mixture of long-chain acids (monounsaturated fatty acids (MUFA), polyunsaturated fatty acids (PUFA), and saturated fatty acids), fatty acid esters and amines, N-heterocyclic compounds, and others. The relative peak areas from the GC−MS results are shown in Table S2.

The highest concentrations in the biocrude oil from both feedstocks were long-chain acids, with MUFA and PUFA (9-hexadecenoic acid and octadec-9-enoic acid) and saturated fatty acids (hexadecenoic acid and octadecanoic acid) likely formed during hydrolysis of triacylglycerides.[31] Compared to SDW, the biocrude oil from GFW also contained a significant amount of fatty acid esters and amines (9-octadecenamide, hexadecenoic ethyl ester, and oleic diethanolamide) from the recombination of lipids and amines from the degraded protein in the more nitrogen-rich GFW feedstock. Notably, the relative peak areas obtained from GC−MS only provide a qualitative estimate of compounds within the HTL biocrude oil, as a large fraction of oil compounds that are high molecular weight, especially cyclic aromatics with heteroatoms, cannot volatilize at temperatures suitable for GC−MS detection.[38]

The physicochemical compositions for the two types of biocrude oil could provide insight into strategizing necessary downstream biocrude oil upgrading processes in future work, including dewatering, desalting, and demetallization to prevent corrosion and catalyst deactivation, along with hydrotreating to

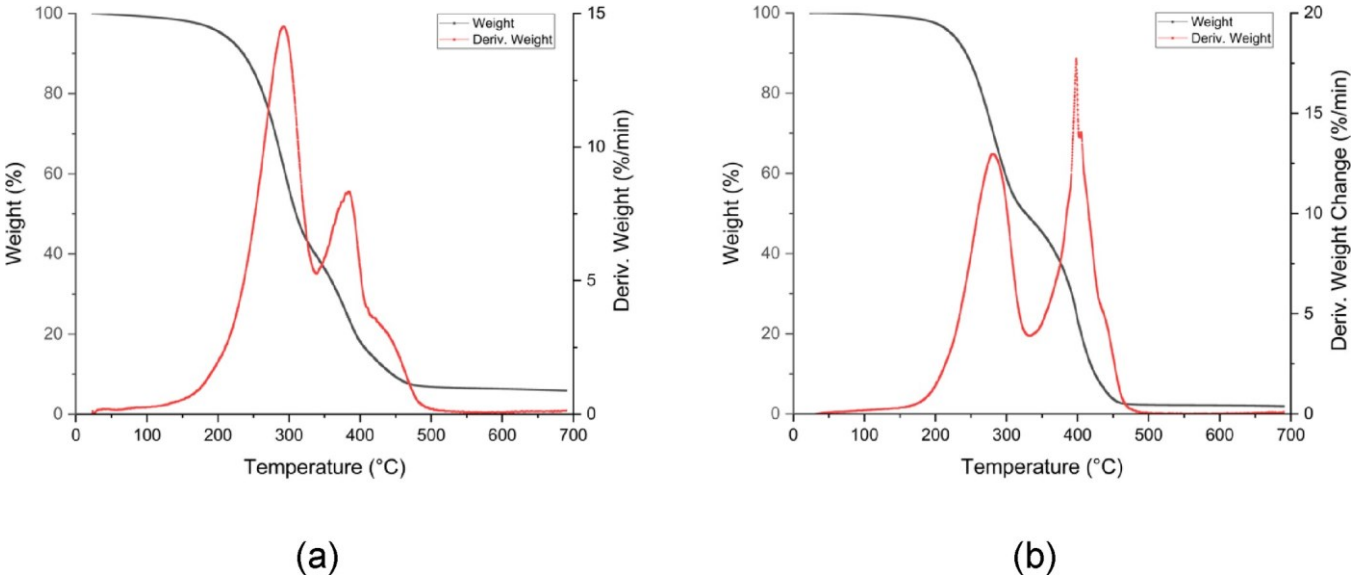

Figure 6. TGA and DTG curves of HTL biocrude oil from (a) GFW and (b) SDW.

https://doi.org/10.1021/acs.iecr.3c01587
Ind. Eng. Chem. Res. 2023, 62, 12174−12182

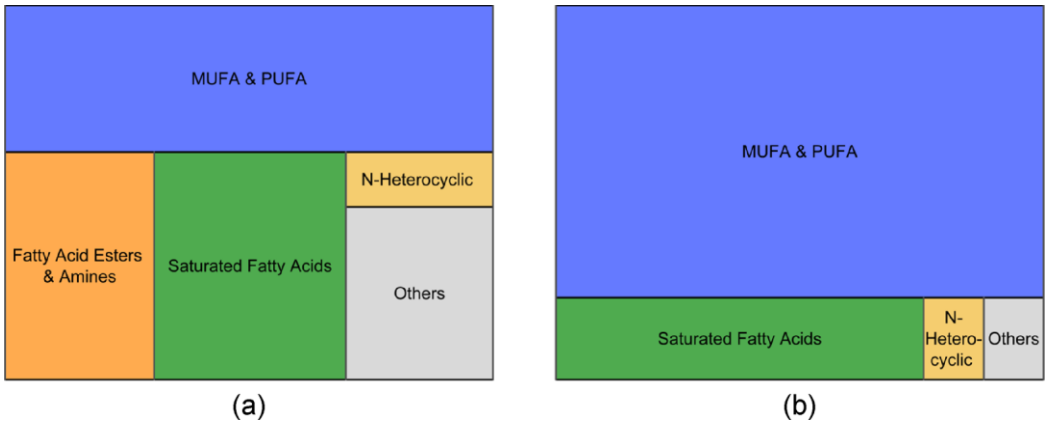

Figure 7. Relative peak area of chemical compounds detected with GC−MS for HTL biocrude oil from (a) GFW and (b) SDW.

remove undesirable nitrogen and oxygen retained in the biocrude oil.

4. CONCLUSIONS

Pilot-scale HTL reactor development and performance evaluation is a critical step toward commercialization of the technology. This paper described the development and performance of a mobile pilot-scale HTL reactor that processed two types of food wastes. High biocrude oil yields were obtained (>47 wt %), along with high energy recovery (>68%) and carbon recovery (>65%). However, high retention of undesirable elements was observed in the biocrude oil from SDW feedstock due to its high lipid content. This pilot-scale HTL reactor yielded an ample amount of biocrude oil and PHW to allow for downstream research on upgrading for transportation fuel and PHW treatment and nutrient reuse. The biocrude oil yield, energy, and carbon recovery efficiency obtained from this study can also provide pilot-scale data for technoeconomic analysis of HTL technology.

ASSOCIATED CONTENT

Supporting Information

The Supporting Information is available free of charge at https://pubs.acs.org/doi/10.1021/acs.iecr.3c01587.

Additional data for the characterization of PHW and biocrude oil from the pilot-scale HTL reactor (PDF)

AUTHOR INFORMATION

Corresponding Author

Yuanhui Zhang − *Department of Agricultural and Biological Engineering, University of Illinois at Urbana−Champaign, Urbana, Illinois 61801, United States*; orcid.org/0000-0003-1387-5618; Email: yzhang1@illinois.edu

Authors

Sabrina Summers − *Department of Agricultural and Biological Engineering, University of Illinois at Urbana−Champaign, Urbana, Illinois 61801, United States*

Amanda Valentine − *Department of Agricultural and Biological Engineering, University of Illinois at Urbana−Champaign, Urbana, Illinois 61801, United States*

Zixin Wang − *Department of Agricultural and Biological Engineering, University of Illinois at Urbana−Champaign, Urbana, Illinois 61801, United States*

Complete contact information is available at: https://pubs.acs.org/10.1021/acs.iecr.3c01587

Notes

The authors declare no competing financial interest.

ACKNOWLEDGMENTS

The authors wish to acknowledge the following funding agencies for the support in various parts of this research: National Science Foundation (CBET 18-04453), Department of Energy (00581194), U.S. Army Engineer Research and Development Center (W9132T-21-2-0009), and the National Science Foundation Graduate Research Fellowship Program. Any opinions, findings, and conclusions or recommendations expressed in this material are those of the authors and do not necessarily reflect the views of the sponsors. The authors thank the University of Illinois Materials Research Laboratory Central Research Facilities and School of Chemical Sciences Microanalysis Laboratory for use of their facilities.

REFERENCES

(1) DOE BETO. *Biofuels and Bioproducts from Wet and Gaseous Waste Streams: Challenges and Opportunities*; Washington D.C., 2017.

(2) Chen, W. T.; Zhang, Y.; Lee, T. H.; Wu, Z.; Si, B.; Lee, C. F. F.; Lin, A.; Sharma, B. K. Renewable Diesel Blendstocks Produced by Hydrothermal Liquefaction of Wet Biowaste. *Nat. Sustainable* 2018, *1* (11), 702−710.

(3) Collett, J. R.; Billing, J. M.; Meyer, P. A.; Schmidt, A. J.; Remington, A. B.; Hawley, E. R.; Hofstad, B. A.; Panisko, E. A.; Dai, Z.; Hart, T. R.; Santosa, D. M.; Magnuson, J. K.; Hallen, R. T.; Jones, S. B. Renewable Diesel via Hydrothermal Liquefaction of Oleaginous Yeast and Residual Lignin from Bioconversion of Corn Stover. *Appl. Energy* 2019, *2019* (233−234), 840−853.

(4) Hietala, D. C.; Godwin, C. M.; Cardinale, B. J.; Savage, P. E. The Independent and Coupled Effects of Feedstock Characteristics and Reaction Conditions on Biocrude Production by Hydrothermal Liquefaction. *Appl. Energy* 2019, *2019* (235), 714−728.

(5) Basar, I. A.; Liu, H.; Carrere, H.; Trably, E.; Eskicioglu, C. A Review on Key Design and Operational Parameters to Optimize and Develop Hydrothermal Liquefaction of Biomass for Biorefinery Applications. *Green Chem.* 2021, *23* (4), 1404−1446.

(6) Elliott, D. C.; Biller, P.; Ross, A. B.; Schmidt, A. J.; Jones, S. B. Hydrothermal Liquefaction of Biomass: Developments from Batch to Continuous Process. *Bioresour. Technol.* 2015, *178*, 147−156.

(7) Watson, J.; Wang, T.; Si, B.; Chen, W. T.; Aierzhati, A.; Zhang, Y. Valorization of Hydrothermal Liquefaction Aqueous Phase: Pathways towards Commercial Viability. *Prog. Energy Combust. Sci.* 2020, *77*, No. 100819.

(8) Li, H.; Lu, J.; Zhang, Y.; Liu, Z. Hydrothermal Liquefaction of Typical Livestock Manures in China: Biocrude Oil Production and Migration of Heavy Metals. *J. Anal. Appl. Pyrolysis* 2018, *135* (September), 133−140.
(9) Tian, C.; Li, B.; Liu, Z.; Zhang, Y.; Lu, H. Hydrothermal Liquefaction for Algal Biorefinery: A Critical Review. *Renewable Sustainable Energy Rev.* 2014, *38*, 933−950.
(10) Toor, S. S.; Rosendahl, L.; Rudolf, A. Hydrothermal Liquefaction of Biomass: A Review of Subcritical Water Technologies. *Energy* 2011, *36* (5), 2328−2342.
(11) Li, H.; Liu, Z.; Zhang, Y.; Li, B.; Lu, H.; Duan, N.; Liu, M.; Zhu, Z.; Si, B. Conversion Efficiency and Oil Quality of Low-Lipid High-Protein and High-Lipid Low-Protein Microalgae via Hydrothermal Liquefaction. *Bioresour. Technol.* 2014, *154*, 322−329.
(12) Anastasakis, K.; Biller, P.; Madsen, R.; Glasius, M.; Johannsen, I. Continuous Hydrothermal Liquefaction of Biomass in a Novel Pilot Plant with Heat Recovery and Hydraulic Oscillation. *Energies* 2018, *11* (10), 2695−23.
(13) Biller, P.; Madsen, R. B.; Klemmer, M.; Becker, J.; Iversen, B. B.; Glasius, M. Effect of Hydrothermal Liquefaction Aqueous Phase Recycling on Bio-Crude Yields and Composition. *Bioresour. Technol.* 2016, *220*, 190−199.
(14) Li, H.; Zhu, Z.; Lu, J.; Watson, J.; Kong, D.; Wang, K.; Zhang, Y.; Liu, Z. Establishment and Performance of a Plug-Flow Continuous Hydrothermal Reactor for Biocrude Oil Production. *Fuel* 2020, *280* (June), No. 118605.
(15) Mørup, A. J.; Becker, J.; Christensen, P. S.; Houlberg, K.; Lappa, E.; Klemmer, M.; Madsen, R. B.; Glasius, M.; Iversen, B. B. Construction and Commissioning of a Continuous Reactor for Hydrothermal Liquefaction. *Ind. Eng. Chem. Res.* 2015, *54* (22), 5935−5947.
(16) Beims, R. F.; Hu, Y.; Shui, H.; Xu, C. Hydrothermal Liquefaction of Biomass to Fuels and Value-Added Chemicals: Products Applications and Challenges to Develop Large-Scale Operations. *Biomass Bioenergy* 2020, *135* (July 2019), No. 105510.
(17) Johannsen, I.; Kilsgaard, B.; Milkevych, V.; Moore, D. Design, Modelling, and Experimental Validation of a Scalable Continuous-Flow Hydrothermal Liquefaction Pilot Plant. *Processes* 2021, *9* (2), 234−18.
(18) Hu, S.; Luo, X.; Li, Y. Polyols and Polyurethanes from the Liquefaction of Lignocellulosic Biomass. *ChemSusChem* 2014, *7* (1), 66−72.
(19) WANG, M.; XU, C.; LEITCH, M. Liquefaction of Cornstalk in Hot-Compressed Phenol-Water Medium to Phenolic Feedstock for the Synthesis of Phenol-Formaldehyde Resin. *Bioresour. Technol.* 2009, *100* (7), 2305−2307.
(20) Feng, S.; Yuan, Z.; Leitch, M.; Xu, C. C. Adhesives Formulated from Bark Bio-Crude and Phenol Formaldehyde Resole. *Ind. Crops Products* 2015, *76*, 258−268.
(21) Ghadge, R.; Nagwani, N.; Saxena, N.; Dasgupta, S.; Sapre, A. Design and Scale-up Challenges in Hydrothermal Liquefaction Process for Biocrude Production and Its Upgradation. *Energy Convers. Manage.: X* 2022, *14* (April), No. 100223.
(22) Castello, D.; Pedersen, T. H.; Rosendahl, L. A. Continuous Hydrothermal Liquefaction of Biomass: A Critical Review. *Energies* 2018, *11* (11), 3165.
(23) Summers, S.; Yang, S.; Watson, J.; Zhang, Y. Diesel Blends Produced via Emulsification of Hydrothermal Liquefaction Biocrude from Food Waste. *Fuel* 2022, *324*, No. 124817.
(24) He, B. J.; Zhang, Y.; Yin, Y.; Funk, T. L.; Riskowski, G. L. Operating Temperature and Retention Time Effects on the Thermochemical Conversion Process of Swine Manure. *Trans. ASAE* 2000, *43* (6), 1821−1825.
(25) He, B. J.; Zhang, Y.; TFunk, T. L.; Riskowski, G. L.; Yin, Y. Thermochemical Conversion of Swine Mamure: An Alternative Process for Waste Treatment and Renewable Energy Production. *Trans. ASAE* 2000, *43* (6), 1827−1833.
(26) He, B. J.; Zhang, Y.; Yin, Y.; Funk, T. L.; Riskowski, G. L. Preliminary Characterization of Raw Oil Products from the Thermochemical Conversion of Swine Manure. *Trans. ASAE* 2001, *44* (6), 1865−1871.
(27) He, B.; Zhang, Y.; Yin, Y.; Funk, T.L.; Riskowski, G. L. Effects of Feedstock PH, Initial CO Addition, and Total Solids Content on the Thermochemical Conversion Process of Swine Manure. *Trans. ASAE* 2001, *44* (3), 697−701.
(28) Ocfemia, K. S.; Zhang, Y.; Funk, T. Hydrothermal Processing of Swine Manure into Oil Using a Continuous Reactor System: Development and Testing. *Trans. ASABE* 2006, *49* (2), 533−541.
(29) Ocfemia, K. S.; Zhang, Y.; Funk, T. Hydrothermal Processing of Swine Manure to Oil Using a Continuous Reactor System: Effects of Operating Parameters on Oil Yield and Quality. *Transact. ASABE* 2006, *49* (6), 1897−1904.
(30) Minarick, M.; Zhang, Y.; Schideman, L.; Wang, Z.; Yu, G.; Funk, T.; Barker, D. Product and Economic Analysis of Direct Liquefaction of Swine Manure. *Bioenerg. Res.* 2011, *4* (4), 324−333.
(31) Aierzhati, A.; Watson, J.; Si, B.; Stablein, M.; Wang, T.; Zhang, Y. Development of a Mobile, Pilot Scale Hydrothermal Liquefaction Reactor: Food Waste Conversion Product Analysis and Techno-Economic Assessment. *Energy Convers. Manag.: X* 2021, *10*, No. 100076.
(32) Watson, J.; Si, B.; Wang, Z.; Wang, T.; Valentine, A.; Zhang, Y. Towards Transportation Fuel Production from Food Waste: Potential of Biocrude Oil Distillates for Gasoline, Diesel, and Jet Fuel. *Fuel* 2021, *301* (March), No. 121028.
(33) ASTM International. ASTM D2892-20: Standard Test Method for Distillation of Crude Petroleum (15-Theoretical Plate Column). *Annual Book of ASTM Standards*. ASTM International; 2020. https://doi.org/10.1520/mnl10903m.
(34) ASTM International. ASTM D974-14: Standard Test Method for Acid and Base Number by Color-Indicator Titration. *Annual Book of ASTM Standards*; ASTM International. 201417. https://doi.org/10.1520/D0974-14.
(35) Speight, J. G. *Handbook of Petroleum Product Analysis*; John Wiley & Sons, Inc., 2002; Vol. *53*.
(36) *NIST Chemistry WebBook, NIST Standard Reference Database Number 8*; Linstrom, P. J., Mallard, W. G., Eds.; National Institute of Standards and Technology: Gaithersburg. https://doi.org/10.18434/T4D303.
(37) Ouadi, M.; Bashir, M. A.; Speranza, L. G.; Jahangiri, H.; Hornung, A. Food and Market Waste-A Pathway to Sustainable Fuels and Waste Valorization. *Energy Fuels* 2019, *33* (10), 9843−9850.
(38) Vardon, D. R.; Sharma, B. K.; Scott, J.; Yu, G.; Wang, Z.; Schideman, L.; Zhang, Y.; Strathmann, T. J. Chemical Properties of Biocrude Oil from the Hydrothermal Liquefaction of Spirulina Algae, Swine Manure, and Digested Anaerobic Sludge. *Bioresour. Technol.* 2011, *102* (17), 8295−8303.
(39) Fan, Y.; Hornung, U.; Raffelt, K.; Dahmen, N. The Influence of Lipids on the Fate of Nitrogen during Hydrothermal Liquefaction of Protein-Containing Biomass. *J. Anal. Appl. Pyrolysis* 2020, *147* (February), No. 104798.
(40) Ren, R.; Han, X.; Zhang, H.; Lin, H.; Zhao, J.; Zheng, Y.; Wang, H. High Yield Bio-Oil Production by Hydrothermal Liquefaction of a Hydrocarbon-Rich Microalgae and Biocrude Upgrading. *Carbon Resour. Convers.* 2018, *1* (2), 153−159.
(41) Cheng, F.; Cui, Z.; Mallick, K.; Nirmalakhandan, N.; Brewer, C. E. Hydrothermal Liquefaction of High- and Low-Lipid Algae: Mass and Energy Balances. *Bioresour. Technol.* 2018, *2018* (258), 158−167.

https://doi.org/10.1021/acs.iecr.3c01587
Ind. Eng. Chem. Res. 2023, 62, 12174−12182